DESIGN AND PERFORMANCE OF FLASHLAMP-PUMPED ND:GLASS AMPLIFIERS FOR THE NIF*

A. C. Erlandson   C. Marshall   M. Rotter   O. Carbourdin**   G. LeTouze**

T. Alger   E. Moor   S. Sutton   E. Grebot**   X. Maille**

J. Horvath   L. Pedrotti   L. Zapata   J. Guenet**   S. Seznec**

K. Jancaitis   S. Rodriguez   J. Beullier**   M. Guenet**

The National Ignition Facility (NIF) will use a 192-beam, 1.8-MJ laser for inertial confinement fusion (ICF) experiments.[1] A major laser component of the NIF, the flashlamp-pumped Nd:glass amplifiers must provide sufficient gain and stored energy to meet requirements for laser energy and power while adding minimal wavefront distortion to the laser beams. The NIF amplifiers differ from those used in previous ICF laser systems mainly in their overall scale and packaging. Figure 1 shows a two-slab-long, 4 × 2 NIF amplifier module, where the n × m designation denotes the number (height × width) of parallel amplifying channels or beam apertures that are combined. The NIF amplifiers use 40-cm-square apertures, which approximate the practical size limit imposed by amplified spontaneous emission (ASE) that depumps the laser slabs and limits gain. Large-aperture size reduces system costs by reducing the number of laser beams needed to produce the required energy on target. Previously, the largest amplifiers constructed were the 2 × 2 Beamlet amplifiers, which combined only four 40-cm-square apertures.[2]

Amplifiers with combined beams were first proposed by Lawrence Livermore National Laboratory (LLNL) in 1978 as a way of reducing the cost of MJ-class fusion laser systems.[3] Combining beams in a single enclosure reduces costs in three ways: (1) by making amplifiers more compact, thereby reducing the size and cost of the building; (2) by increasing pumping efficiency, thereby reducing the size and cost of the power-conditioning system; and (3) by reducing the number of internal amplifier parts. The NIF design achieves considerable cost savings by making the NIF amplifiers larger than the Beamlet amplifiers. Similar amplifiers will be used in the Laser Megajoule (LMJ), a 240-beam laser system now being developed and designed by the French Commissariat a l'Energie Atomique (CEA). Much of the development work for the LMJ amplifiers resulted from collaborative efforts between scientists and engineers at LLNL and the French CEA.

FIGURE 1. A two-slab-long, 4 × 2 NIF amplifier module.   (70-00-0199-0056pb02)

This article describes the design and performance of the NIF amplifiers. First, we describe the NIF amplifier design. Next, we describe the prototype amplifier we tested and discuss the equipment used to measure its optical performance. We then compare model predictions with measurement results, and show performance predictions for the NIF amplifiers that are based on our test results and validated models.

NIF Amplifier Design

Pump Cavity Design and Performance

The NIF amplifiers provide optical gain at the 1.053-μm wavelength by using neodymium-doped, phosphate glass, rectangular laser slabs oriented at Brewster's angle with respect to the beam, to eliminate reflection losses. The slabs have absorbing glass edge claddings to prevent internal parasitic laser oscillation. Each slab holder supports four slabs, one stacked above the other. Central flashlamps cassettes pump slabs in both directions, while side flashlamp cassettes with large silver reflectors pump slabs in one direction. The glass blastshields between the flashlamps and the laser slabs serve three purposes: (1) they prevent acoustic waves generated by the flashlamps from propagating into the beam path and causing wavefront distortion; (2) they provide a contamination barrier between the flashlamp cavity and the critical slab cavity; and (3) they form one wall of the channel used for flowing cooling gas around the flashlamps. Figure 2 shows a plan view of a single NIF amplifier slab column that illustrates the arrangement of the slabs, flashlamps, blast shields, and reflectors.

The NIF amplifiers must meet requirements for gain, gain uniformity, wavefront distortion, and thermal recovery rate. High gain is required for the laser to meet its output energy and power requirements, especially because of the limited injected-energy from an affordable pulse generation system. At the same time, the amplifier must achieve its gain requirements efficiently to reduce the size and cost of the power-conditioning system used to drive the flashlamps. Accordingly, the NIF amplifiers use several features to increase efficiency. The side flashlamp arrays use silver reflectors

FIGURE 2. Plan view of the NIF amplifier pump cavity. (70-00-0199-0057pb02)

Side flashlamp cassette

Lamp   Ag

AR-coated blast shield

Central flashlamp cassette
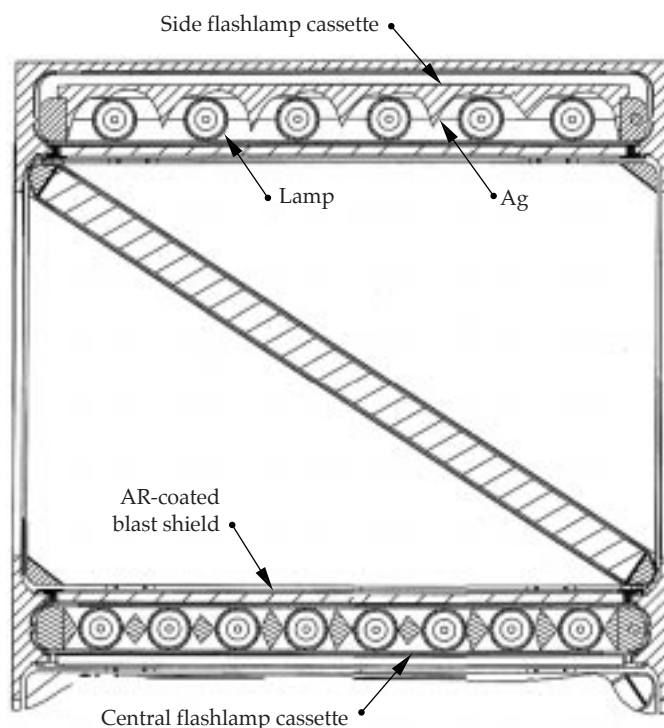
with involute reflector shapes. They are designed to reflect flashlamp light toward the laser slabs, while returning little flashlamp light back to the absorbing flashlamp plasma.[4] Compared with flat reflectors, the involute reflectors reduce the flashlamp electrical energy required to meet the gain requirement by ~15%. Additional reductions in flashlamp electrical energy are achieved by using sol-gel antireflective (AR) coatings on both sides of the blast shields (7%) and by preionizing the flashlamps with weak electrical pulses delivered several hundred microseconds before the main pulse (10%). Preionization causes the flashlamp arc to develop more uniformly, and it increases the electrical-to-optical conversion efficiency of the flashlamp plasma. Overall, the predicted storage efficiency of the NIF amplifiers is 3.8%, which is significantly higher than those in previous ICF lasers (3.0% and 1.8% for the Beamlet and Nova amplifiers, respectively).[2] Storage efficiency is defined as the total extractable energy stored in the laser slabs divided by the electrical energy delivered to the flashlamps.

In addition to the above criteria, we want the amplifiers to produce uniform gain distributions across their apertures, so that uniform beam output fluence can be readily obtained. Uniform output fluence is essential for maximizing output energy while maintaining acceptable optical damage risk. With significant gain variations, it becomes necessary to compensate by increasing the input fluence distribution in regions of the aperture with lower gain, as was done on the Beamlet laser. In large slabs, such as the 4.1- × 45.8- × 80.9-cm slabs used in the NIF amplifiers, the transverse gain uniformity is determined not only by the distribution of flashlamp light across the slab, but also by internal amplified spontaneous emission. ASE preferentially depletes gain near the slab's ends because this position has the longest path length for internal amplification.[2,5] The skewed diamond-shaped reflectors in the central flashlamp arrays reduce gain variations in the NIF pump-cavity design by directing flashlamp light preferentially near the slab ends.

We used a 3D ray-trace code to evaluate reflector shapes and to predict gain distributions across the aperture. The 3D code calculates pump rates for the neodymium-ion inversion by using a reverse ray-trace technique where rays were propagated backward from the point of interest in the slab to the flashlamp plasma. The ray-trace model tracked the change in the spectral content of each ray as it interacts with various reflecting and transmitting media present in the pump cavity. The absorption and reflectance properties of cavity components and the emission properties of the lamp plasma were determined experimentally.[6] Once the pump distribution was calculated as a function of flashlamp power, the peak gain-coefficient distribution was calculated by solving the differential equation for stored energy density as a function of time at each point in the slab. In addition to radiative and nonradiative spontaneous decay processes, the model also tracked spatially and temporally dependent ASE decay rates throughout the volume of the laser slabs. Both the physical assumptions in the model and the calculational techniques used in the computer programs that implement the gain model have been described in detail in earlier publications.[7,8,9]

Wavefront distortion is produced by waste heat deposited in the laser slabs by flashlamp pumping processes. Wavefront distortion has a prompt component that is caused by the flashlamp heating the laser slabs during the shot; it also has a residual thermal component that is caused by thermal energy remaining in the pump cavity from previous shots. The prompt component is primarily caused by the uneven heating of the two sides of the slab. This causes the slab to warp before the laser beam passes through the slabs when peak gain is attained.[10] Residual thermal distortions are caused by thermal gradients in the laser slabs themselves, as well as thermal gradients in the gas that is convectively heated by the laser slabs. The residual slab distortions, like the prompt pump-induced distortion, tend to be low order. The deformable mirror system now planned for the NIF is expected to correct the residual slab distortions. The gas distortions, however, have higher spatial frequencies and are more rapidly varying, making them difficult to correct.

To accelerate the recovery from residual thermal distortion, the NIF flashlamps will be actively cooled by flowing gas. Flashlamp cooling is effective because some 60% of the pump waste heat resides in the flashlamp envelopes immediately after a shot. Although water cooling has been successfully used to accelerate the shot rate of the OMEGA Laser at the University of Rochester,[11] gas cooling was chosen for the NIF to eliminate water-jacket tubes and to leave more room for efficiency-enhancing reflectors. NIF flashlamp cooling system will provide gas flow rates of up to 20 cubic feet per minute per flashlamp, with the gas flow direction alternating between flashlamp cassettes as shown in Figure 3. The inlet temperature of the cooling gas will be controlled over a ±5°C range centered about the ambient temperature with ±0.3°C accuracy.

We used several computer codes to calculate the wavefront distortion induced by flashlamp pumping processes. The prompt temperature rise, which was assumed to be proportional to the time-integrated local pump rate, was calculated using a 2D ray-trace code, which was a precursor to the 3D ray-trace code described above.[12] The residual temperature component was calculated using a finite-element heat transfer program, with starting temperatures set equal to values measured on a

test amplifier shortly after firing the flashlamps.[13] The calculated temperature distributions were used as input for finite-element calculations of the deformation and stress in the laser slabs.[14] The final step in the calculation sequence was to use the calculated temperature, deformation, and stress distributions in a ray-trace algorithm to evaluate the optical path length variations across the aperture.[15] The effects of refractive index responses to temperature and stress were included in the calculations.

Mechanical Design

The large scale of the NIF amplifiers requires new mechanical designs that allow convenient assembly and maintenance. Accordingly, the NIF amplifiers use a modular design in which the most critical components, including the flashlamps, laser slabs, and reflectors, are mounted in line-replaceable units or cassettes that can be readily inserted or removed without disturbing their neighbors.[16] See Figure 4.

The design uses sealed maintenance carts that access the bottom of the amplifiers in order to install and remove flashlamp cassettes and four-high slab cassettes. The cassettes are inserted and removed from their enclosure, called the frame assembly unit, which is supported by top plates mounted to an overhead support structure. Plenums distribute electricity and cooling gas to the flashlamps from the top, through holes on the top plate.

Each NIF 4 × 2 beam bundle uses an 11-slab-long main amplifier that the beam passes four times, and a five-slab-long power amplifier that the beam passes twice. Assembly of these amplifiers begins in an off-line clean room, where the frame assembly units are cleaned and the top plates and blast shields with antireflective coatings are installed. A flashlamp-light-resistant polymer is used to bond the blast shields to a metal frame, and silicone inflatable seals are used to seal the metal frame to the inside of the frame assembly unit. These seals reduce leak rates between the flashlamp cavity and the slab cavity. After the blast shields have been installed, frame assembly units are bolted together to form 5- and 11-slab-long units that are
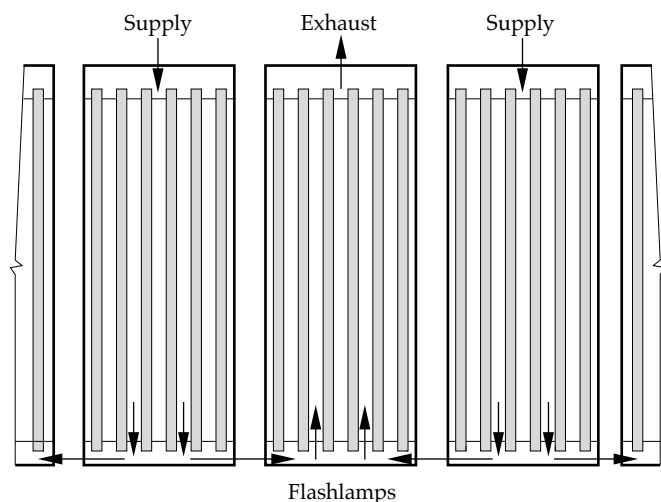

FIGURE 3. Alternating the direction of cooling gas flow through the flashlmp cassettes enabled us to put cooling-gas connections at the top of the amplifier, thereby simplifying the amplifier mechanical design.   (70-00-0199-0058pb02)
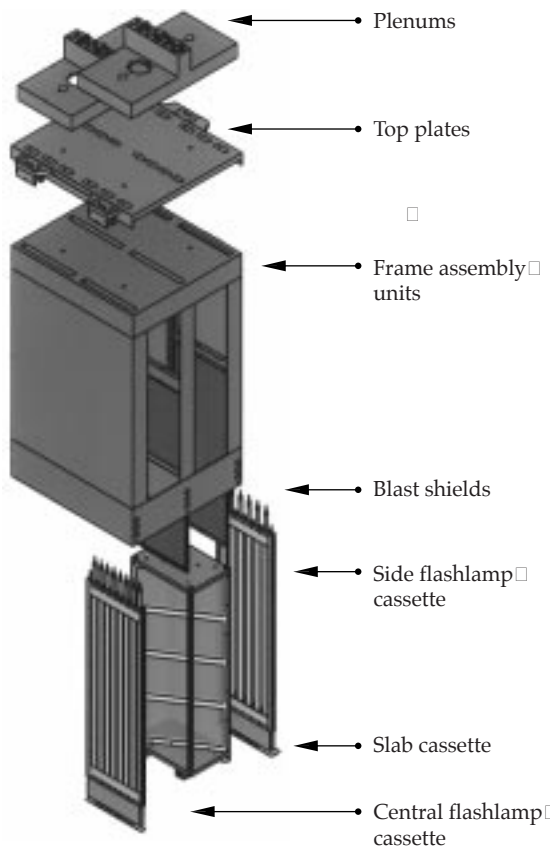
Plenums

Top plates

Frame assembly units

Blast shields

Side flashlamp cassette

Slab cassette

Central flashlamp cassette

FIGURE 4. The NIF amplifiers use a modular design. (70-00-0199-0059pb02)

the cart and the bottom cover of the frame assembly unit have been pressed together to trap residual particles, the cover pair is moved to the side to open a passageway for the slab cassette to be raised into the frame assembly unit. Rollers mounted in the corners of the cassette guide the cassette during insertion and prevent metal-on-metal rubbing, which generates particles. A fail-safe mechanism in the cart activates latches that hold the slab cassette in place. Slab cassettes can be removed for occasional refurbishment by reversing this installation process. Figure 5 shows a prototype slab cassette cart, which has successfully completed some 50 slab-cassette transfers in our laboratory. Similar carts will be used to install and remove the NIF flashlamp cassettes and blast shields.

transported to the laser bay where they are mounted to an overhead support structure by their top plates.

The laser slabs, reflectors, and metal parts that comprise the slab cassettes are spray-cleaned and assembled in an elevated, class-100 clean room. We have to maintain high cleanliness levels because small particles resting on the laser slabs can cause damage when heated by flashlamp and laser light. Current specifications call for the laser slabs and metal surfaces to be maintained at cleanliness levels of 50 and 100, respectively. The levels correspond to particle-size distributions in which there are only one 50- or 100-μm particle per square foot of surface area, respectively. Following assembly, the slab cassettes are lowered into a specialized clean cart. Once the cart has been moved to the laser bay, it docks to the bottom of a frame assembly unit and establishes a hermetic seal to maintain cleanliness. After the top cover of

FIGURE 5. The prototype slab cassette cart shown inserting a slab cassette into the NIF prototype amplifier.   (70-00-0199-0060pb02)

NIF Prototype Amplifier Design

We have built and tested a prototype amplifier at LLNL to validate key requirements prior to deployment in NIF. This prototype amplifier was extremely close to the NIF amplifier design, as it used the same size flashlamps and laser slabs and nearly the same reflector shapes. The prototype amplifier was slightly more compact in the direction transverse to the laser beam because the insertion clearances between the slab cassettes and the frame assembly units are smaller, and the blast shields are thinner. In addition, the prototype was slightly more compact in the direction parallel to the beam due to smaller gaps between frame assembly units. Ray-trace codes that we have developed to predict amplifier gain show that the differences in gain and storage efficiency between the prototype amplifier and the NIF amplifiers are negligible.

The prototype amplifier was tested as a one-, two-, and three-slab-long amplifier. Both the "diamond" and "X" configurations of the two-slab-long amplifier were tested. Amplifiers of different lengths were tested in order to infer the gain and wavefront distributions of the interior slab; this was important because the 5- and 11-slab-long NIF amplifiers have many interior slabs in addition to X and diamond end slabs. Figure 6 shows the diamond, X, and three-slab-long amplifier configurations we tested.

To measure temperatures at approximately 80 different locations inside the amplifier, we used thermocouples. They were placed on three laser slabs in one of the slab cassettes with holes drilled through the slabs to establish good thermal contact. Thermocouples were also placed on flashlamps, blast shields, and reflectors near the slab cassette. The purpose of the temperature measurements was to determine the initial temperature rise of the pump cavity components and to determine cooling rates after shots.
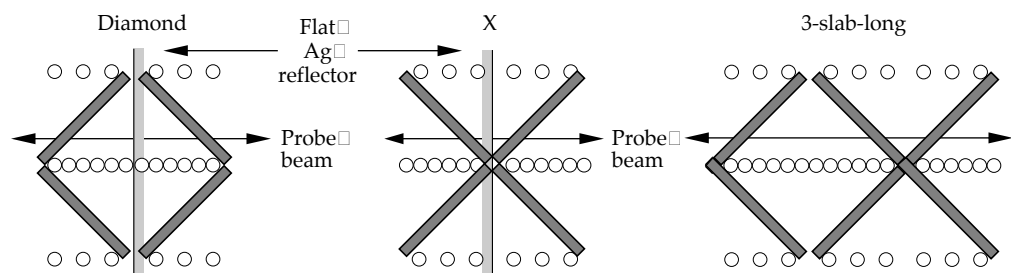
The laser slabs in the prototype amplifier were finished from LG-770 glass made by Schott Glass and LHG-8 glass made by Hoya. Both types of laser glass had Nd ion concentrations of 4.2×10^{20} ions/cm^3. The flashlamps were made by EG&G and ILC Technology.

Apparatus for Gain and Wavefront Measurements

We constructed an optical diagnostic system to perform time-resolved gain and wavefront measurements over the entire aperture of our prototype amplifier. Measurements were performed using a pulsed, injection-seeded, single-longitudinal mode, Nd:YLF probe laser operating at 1.053 μm. This laser produced 80-mJ, 20-ns-long pulses at a repetition rate of 13 Hz. The probe laser beam was expanded and image relayed by a series of telescopes. After passing through the amplifier once, the beam reflected back through the amplifier and telescopes a second time. After returning from the amplifier, a portion of the beam was sampled with a beam splitter and reflected to scientific-grade charge-coupled device (CCD) cameras for gain and wavefront measurements. Figure 7 shows a schematic of our equipment.

Amplifier gain distributions were determined by calculating the ratio of the images produced by two CCD cameras (the gain reference camera and the gain

FIGURE 6. Plan view of the prototype amplifier in the diamond, X, and 3-slab-long configurations. (70-00-0199-0061pb02)
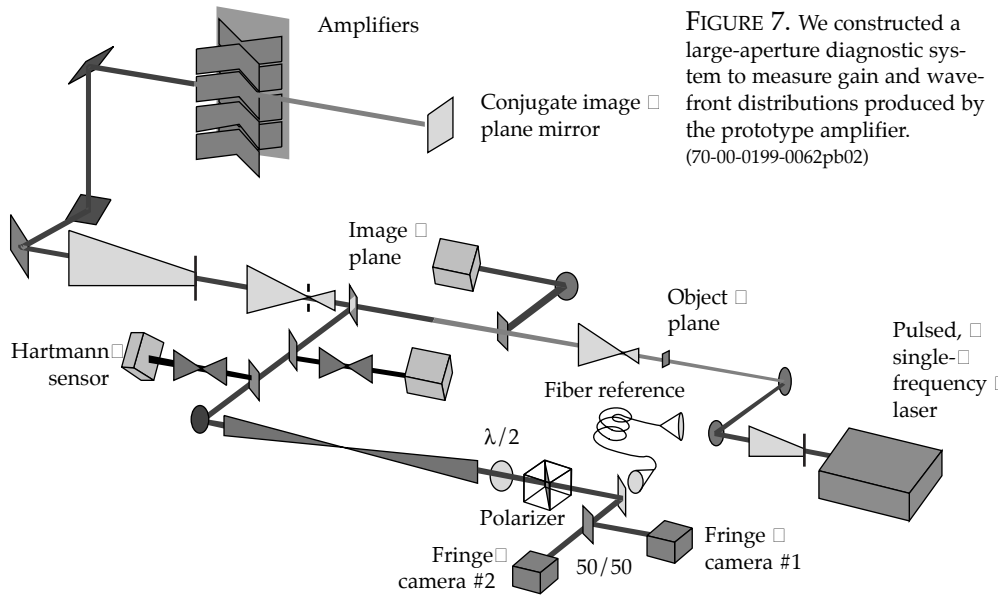
FIGURE 7. We constructed a large-aperture diagnostic system to measure gain and wavefront distributions produced by the prototype amplifier. (70-00-0199-0062pb02)

probe camera); they recorded the laser beam intensity before and after the beam passed through the amplifier. Measured background contributions from the flashlamp light and amplified spontaneous emission were subtracted from the gain camera image. A correction factor for passive transmission losses was determined by firing the probe laser without firing the amplifier flashlamps. Crosshair images were used to ensure proper registration of the gain and reference camera images.

Wavefront distributions were measured by interfering the probe beam with a reference beam, which was generated with an ~25-m-long single-mode optical fiber cut so that its optical length approximately matched the probe laser path length. To increase the fringe contrast ratio, a half-wave plate and a polarizer were used to attenuate the probe laser to approximately the same intensity as the reference beam. Two cameras were used to record interferograms on successive pulses of the 13-Hz probe laser. A Fourier-transform technique was used to calculate wavefront distributions from the interferograms.[17] We checked the calibration of the interferometer by measuring the wavefront of a known lens. From this check, we estimate the accuracy of our wavefront measurements to be ±0.02 waves rms, for both cameras. Prompt pump-induced wavefront distortion was determined by subtracting the wavefront measured at the time of peak gain from the wavefront measured 75 ms earlier.

Measurement Results and Comparison with Model Predictions

Gain measurements were in close agreement with model predictions. For example, Figure 8 shows measured and predicted gain-coefficient distributions for the two-slab-long X configuration, with the flashlamp pulses close to the 34-kJ per lamp, 360-μs-long pulses anticipated for the NIF. Although the distributions in Figure 8 characterize the aperture next to the bottom, distributions measured in the other apertures were nearly the same, due to the vertical translation symmetry of the pump cavity. Gain was lower on the right-hand side of the aperture because the right-hand sides of both slabs were close to the ends of the amplifier where pump-light fluences were lower. Differences between the model predictions and measurements were less than 1% rms for all other combinations of apertures and configurations (diamond, X, and 3-slab-long). This agreement was achieved with a single value of the adjustable parameter used in the model to scale the flashlamp pumping rate.
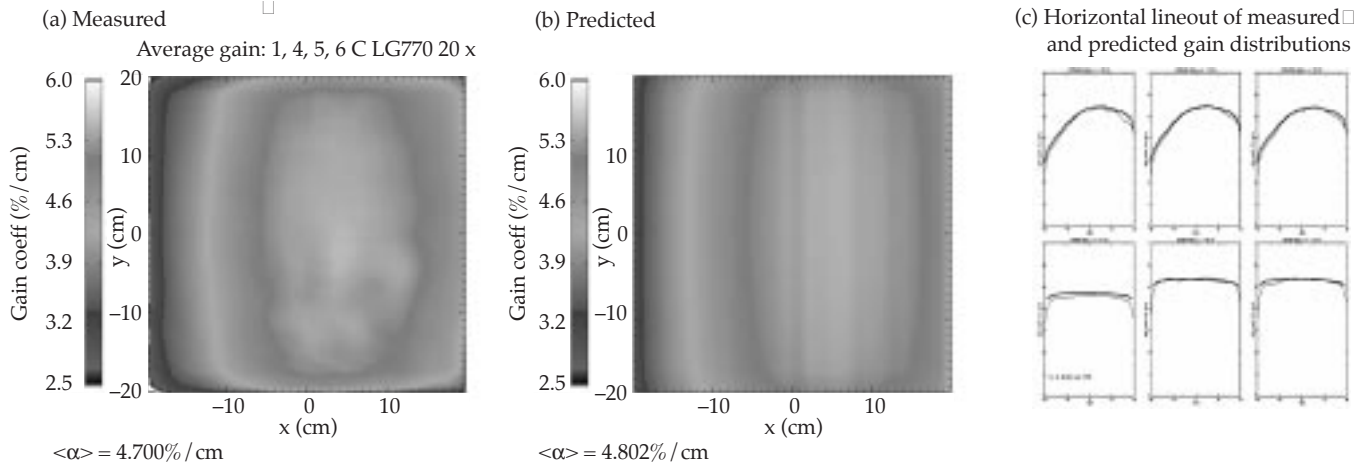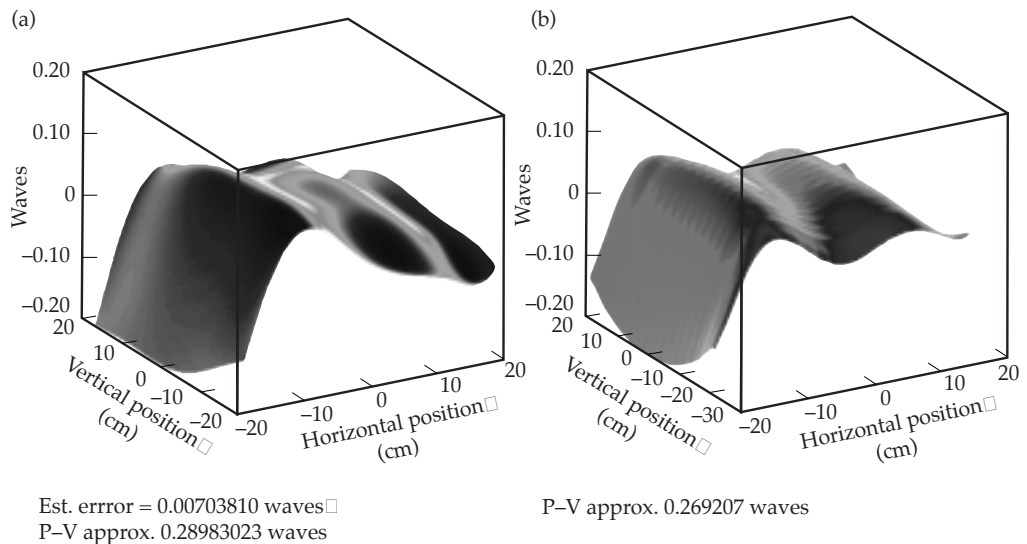
(a) Measured

Average gain: 1, 4, 5, 6 C LG770 20 x

(b) Predicted

(c) Horizontal lineout of measured and predicted gain distributions

$<\alpha> = 4.700\% / \text{cm}$

$<\alpha> = 4.802\% / \text{cm}$

FIGURE 8. Measured and predicted gain distributions for the two-slab-long X configuration, with flashlamps energized with 34-kJ-per-lamp, 360-μs-long pulses. Measurements were made in the next-to-bottom aperture. (70-00-0199-0063pb02)

Prompt pump-induced wavefront distortion measurements were also in close agreement with model predictions. Figure 9 compares the measured and predicted prompt pump-induced wavefront distortion for the X configuration and for the standard flashlamp energy of 34 kJ/lamp. The results have been normalized to a single-slab pass. The close agreement between measurements and predictions was obtained using a scaling factor that adjusts the prompt temperature rise in the slab relative to the calculated pumping rate. Equally close agreement was obtained for other apertures and for time delays of up to 1 ms after the time of peak gain, using a single value for the scaling factor.

In addition to the optical characterizations, we also performed temperature measurements to determine the efficacy of the flashlamp cooling system. Figure 10 shows average slab temperature versus time after a flashlamp shot, for two cases: (1) with flashlamp gas set at ambient temperature; and (2) with the flashlamp cooling gas set 0.5°C below ambient temperature. Our data show that the average slab temperature recovers to within ~0.1°C of

FIGURE 9. (a) Measured and (b) predicted prompt pump-induced wavefront distributions for the two-slab-long "X" configuration, with flashlamps energized with 34-kJ-per-lamp, 360-μs-long pulses. Measurements were made in the next-to-bottom aperture.
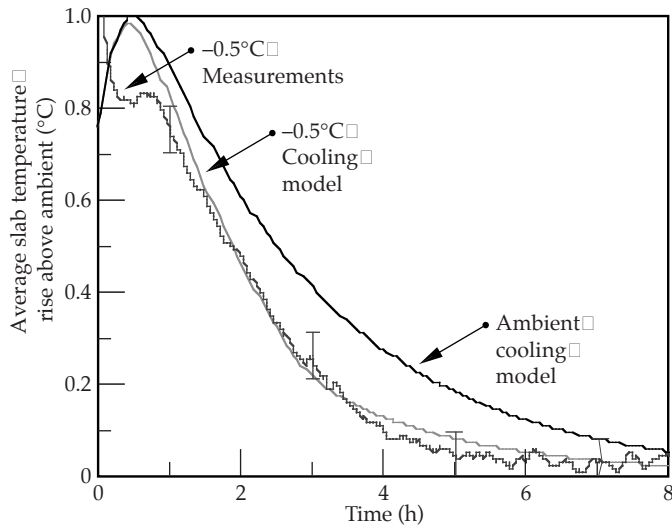
(70-00-0199-0064pb01)

Est. errror = 0.00703810 waves
P–V approx. 0.28983023 waves

P–V approx. 0.269207 waves

FIGURE 10. Using slightly chilled (–0.5°C) cooling gas accelerates slab thermal recovery rates. (70-00-0199-0065pb02)

the ambient temperature in about eight hours using ambient-temperature cooling gas, and in about four hours using slightly chilled gas. Measured gas distortions had high frequency components, with the rms amplitude varying linearly with the difference between the average slab temperature and the ambient temperature. Measured slab distortions were low order and recovered to less than 0.04 waves (peak-to-valley) per slab per pass within 3–4 hours after each shot. This measurement is consistent with the magnitude of the slab distortions, which we expect to correct with a deformable mirror on NIF.

Performance Predictions for the NIF Amplifiers

Figure 11 shows the beamline-averaged gain-coefficient distribution for a NIF laser beam, predicted by our validated 3D ray-trace code. The code took into account several features of the NIF amplifiers that were different from the prototype amplifier: protectively coated Ag reflectors with stable, higher reflectances; improved, two-layer sol-gel antireflective coatings on the blast shields; use of equal numbers of LG-770 and LHG-8 laser slabs; and slight reflector-shape differences. The predicted aperture-averaged gain coefficient was 5.3%/cm, and the distribution

shows the expected gain roll-off near the edges due to ASE. Propagation code modeling of the NIF beamline shows that the gain has sufficient magnitude and uniformity for the NIF laser to meet its beam power and energy requirements. To achieve a uniform output fluence distribution and maximum beam output energy, however, the input fluence distribution of the injected laser beam has to be tailored to compensate for the anticipated gain variations.
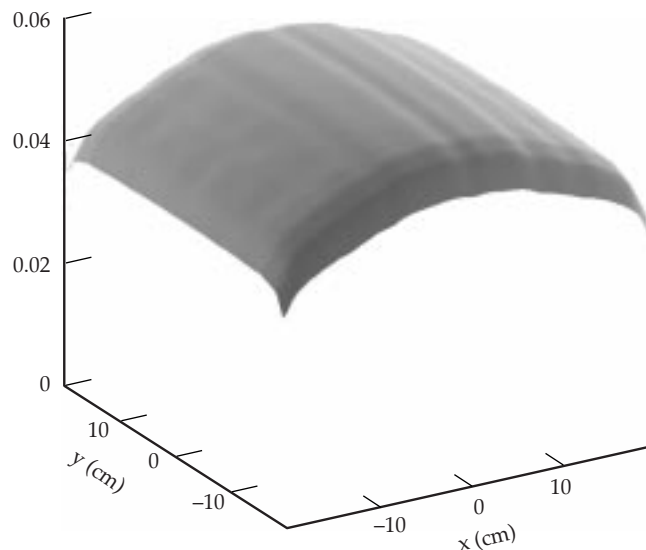

FIGURE 11. NIF beamline-averaged gain-coefficient distribution predicted with the 3D ray-trace code. (70-00-0199-0066pb02)

Figure 12 shows the total prompt pump-induced wavefront distortion for a NIF beamline, predicted with our codes using the source-term scaling factor derived from AMPLAB experiments. The distribution is a low-order "M" shape, with a peak-to-valley value of 5.9 waves. This distribution possibly overestimates the prompt pump-induced wavefront distortion that the NIF beamlines will actually produce, because it is conceivable that stray flashlamp light may have distorted the optics, which are part of the diagnostic. Nonetheless, the predicted distortions are within the range that now appears to be largely correctable with the NIF deformable mirror.

To estimate the effect of the gas distortions on the NIF laser beams, we scaled the gas distortions measured on the prototype amplifier to account for the greater path length and greater number of slabs in the NIF amplifiers. In addition, we used a beam propagation code to calculate the beam focal spot. Our estimate shows that the gas distortions will meet the NIF requirement (less than 5 μrad added beam divergence) within 3 hours after the shot, provided the temperature of the flashlamp cooling gas is ~1°C below the ambient temperature. Figure 13 shows model results for flashlamp cooling with gas at ambient temperature and at 1°C below ambient temperature. The conservative and aggressive estimates correspond to scaling the AMPLAB results by length (for aggressive estimates) and by number of laser slabs (for conservative estimates).
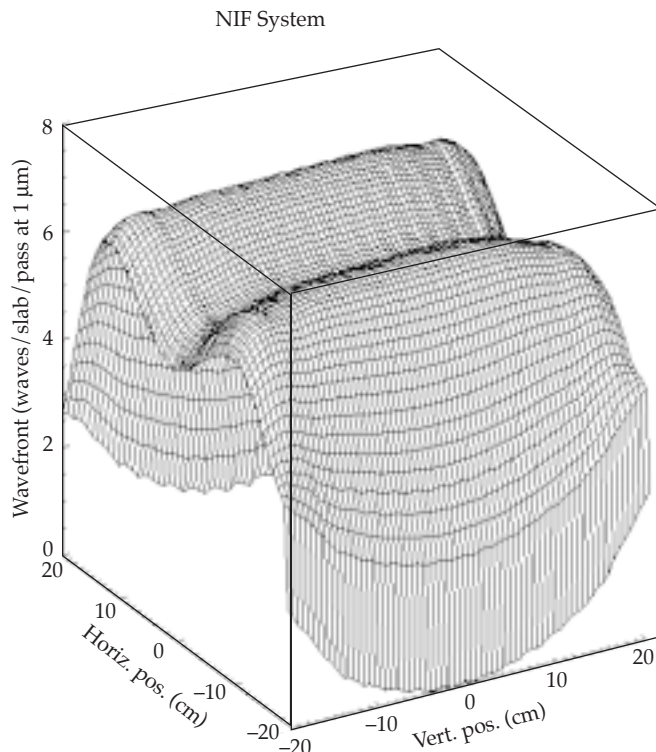

FIGURE 12. NIF beamline prompt pump-induced wavefront distortion predicted with ray-trace and finite-element codes (70-00-0199-0067pb02)
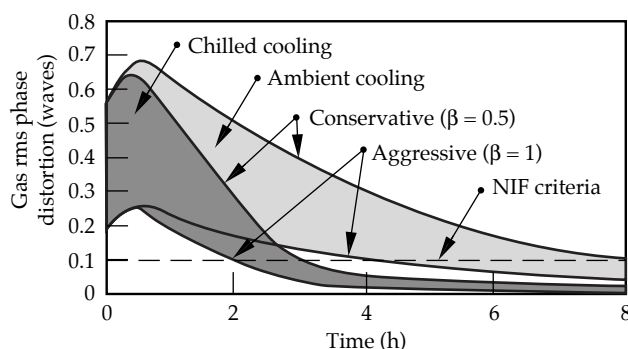

FIGURE 13. Predicted gas-distortion phase distrubances in NIF for ambient and chilled gas cooling. Aggressive and conservative assumptions are used to bracket the problem. (70-00-0199-0068pb02)

Conclusion and Summary

Advances in amplifier technology developed for the NIF include a modular design and bottom-access carts to improve maintenance; features to improve storage efficiency that reduces the size and cost of the power conditioning; and active gas cooling to accelerate the laser shot rate. Further, gain, wavefront, and thermal recovery measurements performed on the NIF prototype amplifier are consistent with meeting NIF performance requirements.

Acknowledgments

Thierry Adjadj,* Gary Ross, John Toeppen, Larry Morris, Jean Lobit,* Douglas Swort, Ronald Bettencourt, Michael Weddle, Loretta Kleinsasser, Dzung Nguyen, John H. Campbell, Daniel Walmer, William Steele, Jerry Britten, Curly Hoagland, Gregory Rogowski, Steve Letts, Cindy Alviso, Irving Stowers, Joe Menapace, Douglas Larson, Scott Hulsey, Phil Test, Steve Fulkerson, George Pollock, Andy Hinz, Anthony Lee, Janice Lawson, Wade Williams, Mark Newton, Ken Manes, Richard London, Yuri Zakharenkhov, Peter Amendt, Jean-Francois Mengue, Fabrisse Laniesse,* John Hunt, John Murray, Richard Hackel, Jeff Paisner, Steve Payne, and Howard Powell.

*Commissariat a L'Energie Atomique (French Atomic Energy Commission)

Notes and References

1. W. H. Lowdermilk, *Second Annual Conference on Solid State Lasers for Application to Inertial Confinement Fusion*, in *Proc. SPIE*, Bellingham, WA, Vol. 3047, p. 16–37 (1997).

2. A. C. Erlandson, M. D. Rotter, D. N. Frank, and R. W. McCracken, *ICF Quarterly Report* **5**(1), 18–28, Lawrence Livermore National Laboratory, Livermore, CA, UCRL-LR-105821-95-1 (1995).

3. W. F. Hagen, *Laser Program Annual Report–1977*, Lawrence Livermore National Laboratory, Livermore, CA, UCRL-50021-77, pp. 2-228 to 2-231 (1978).

4. W. T. Welford and R. Winston, *High Collection Nonimaging Optics,* Academic Press, New York, NY, p. 266 (1989).

5. A. C. Erlandson, K. S. Jancaitis, R. W. McCracken, and M. D. Rotter, *ICF Quarterly Report* **2**(3), 105–114, Lawrence Livermore National Laboratory, Livermore, CA, UCRL-LR-105821-92-3 (1992).

6. H. T. Powell, A. C. Erlandson, and K. S. Jancaitis, Conference on Flashlamp-pumped Laser Technology, in *Proc. SPIE*, Bellingham, WA, Vol. 609, pp. 78–94 (1986).

7. H. T. Powell, A. C. Erlandson, K. S. Jancaitis, and J. E. Murray, *High-Power Solid State Lasers and Applications,* in *Proc. SPIE*, Bellingham, WA, Vol. 1277, pp. 103–120 (1990).

8. K. S. Jancaitis, S. W. Haney, D. H Munro, G. LeTouzé, and O. Cabourdin, in *Proc. SPIE*, Vol. 3047, pp. 106–111 (1997).

9. G. LeTouzé et al., "3-D Gain Modeling of the LMJ and NIF Amplifiers," *Solid State Lasers for Application to Inertial Confinement Fusion*, Third International Conference 1998 (to be published).

10. J. E. Murray, W. F. Hagen, and B. W. Woods, *Laser Programs Annual Report*, UCRL-50021-82, Lawrence Livermore National Laboratory, Livermore, CA, p. 7–72, (1982).

11. J. H. Kelly, M. J. Shoup III, M. D. Skeldon, and S. T. Bui, *Solid State Lasers III*, edited by G. J. Quarles, in *Proc. SPIE*, Bellingham, WA, Vol. 1627, p. 252–259 (1992).

12. G. LeTouzé, O. Cabourdin, J. F. Mengue, M. Rotter, and K. Jancaitis. "Shaped Reflectors for Pump Cavities," *2nd Annual Conf. Solid State Lasers for Application to ICF*, Limeil, France (1996).

13. A. Shapiro, *TOPAZ3D—A 3-D Finite Element Heat Transfer Code*, UCID-20484, Lawrence Livermore National Laboratory, Livermore, CA (1985).

14. B. N. Maker, *NIKE3D—A Nonlinear, Implicit 3-D Finite Element Code for Solid and Structural Mechanics*, UCRL-MA-105268, Rev. 1, Lawrence Livermore National Laboratory, Livermore, CA (1995).

15. S. Doss and R. Gelinas, *Laser Program Annual Report*, UCRL-50021-86, Lawrence Livermore National Laboratory, Livermore, CA, p. 7–132 (1986).

16. A. C. Erlandson et al., *Second Annual Conference on Solid State Lasers for Application to Inertial Confinement Fusion*, in *Proc. SPIE*, Bellingham, WA, Vol. 3047, p. 16–37 (1997).

17. M. Takeda, H. Ina, and S. Kobayashi, *J. Opt. Soc. Am.*, **72**, 156–160 (1982).